photonics

MDPI

Article

Segmented Four-Element Photodiodes in a Three-Dimensional Laser Beam Angle Measurement

Stanislav Konov [1], Aleksander Frolov [1,2], Petr Shapovalov [1,2], Pavel Peretyagin [1,3,*] and Sergey Grigoriev [1]

[1] Department of High-Efficiency Machining Technologies, Moscow State Technological University "STANKIN", 127055 Moscow, Russia; s.konov@stankin.ru (S.K.); a.frolov@stankin.ru (A.F.); p.shapovalov@stankin.ru (P.S.); s.grigoriev@stankin.ru (S.G.)
[2] Department 1030, Central Research Institute of Automation and Hydraulics (CNIIAG), 127018 Moscow, Russia
[3] Scientific Department, A.I. Evdokimov Moscow State University of Medicine and Dentistry, Delegatskaya St., 20, p. 1, 127473 Moscow, Russia
* Correspondence: p.peretyagin@stankin.ru; Tel.: +7-(49)-99732370

Abstract: Based on the registration of two laser beam projections, a method for measuring the angular deviation of a laser beam from its initial position in three-dimensional space is proposed and experimentally demonstrated. The laser ray is directed into the beam-splitting cube, which distributes the ray into two mutually orthogonal parts, on the path of which, two four-segment photodiodes are located at different distances from the beam-splitting cube. The value of the angular deviation from a certain initial position of the laser beam in three-dimensional space is obtained after the mathematical processing of the measured position of the laser beam projections' centers in the photodiodes coordinates systems. The innovation of this method is that the resulting angular deviation of the laser beam is in three-dimensional space due to the registration of a pair of projections. The experimental results also demonstrate that the proposed method has a high speed-measuring potential and can be used for solving a wide range of problems.

Keywords: quadrant slit photodiode; photogrammetry; angular deviation; motion tracking; non-contact measurement

Citation: Konov, S.; Frolov, A.; Shapovalov, P.; Peretyagin, P.; Grigoriev, S. Segmented Four-Element Photodiodes in a Three-Dimensional Laser Beam Angle Measurement. *Photonics* **2023**, *10*, 704. https://doi.org/10.3390/photonics10070704

Received: 11 April 2023
Revised: 14 June 2023
Accepted: 16 June 2023
Published: 21 June 2023

1. Introduction

It is possible to conclude that most modern information-measuring systems are oriented to the solution of contact-coordinate-measuring tasks [1,2]. Usually, the problem statement for a coordinate-measuring system is formulated based on the design and technological limitations of the measured object. Thus, most parts of coordinate measuring, realized nowadays in mechanical engineering, are reduced to control the product elements for the observance of permissible deviations in the dimensions, forms, locations, and microreliefs of different surfaces, set in project documentation [3]. These measurements are supposed to be performed under normal conditions (temperature 20 °C, atmospheric pressure 101.3 kPa, relative humidity 60%, vibration frequency 0.1–30 Hz, vibration amplitude 0.075 mm, and so on).

It should be noted that there is another segment of measuring tasks related to the control of the above parameters in conditions close to the operating conditions of a finished product, i.e., with certain vibrations in different ranges of frequencies and amplitudes, temperature fluctuations, static loads, and other influencing physical factors. Essentially, it is about carrying out full-scale tests on special stands [4] with a realization of the possibility of measuring orientations in space and the linear dimensions of geometrical elements on controlled items.

The urgency of the realization of such measurements is extremely high due to the limited instrumental methods of control that often arise during investigation. For example, in the case of vibration or shock loading, developers have to carry out cycles of vibration loading, measuring only the parameters of the vibration itself, so they have to make judgements about its influence on the geometrical parameters of the investigated object only using the results of the following static measurements of an object by means of coordinate-measuring systems. With such an approach, it is impossible to trace the dynamic deformations of a measured object, which occur only under the action of alternating loads and stopping in an idle condition. More often, in the design of complex lightweight constructions, developers only use the modeling [5] of vibrations and shock loads without carrying out full-scale tests; however, obtaining a new measuring method will allow them to follow the change in the geometrical parameters of the surfaces of the researched objects in the process of their tests and to receive the distribution of the controlled values changing in the process of the research.

In this paper, the authors consider a solution to the problem of tracking, in real time, the spatial position of a certain plane (part of the studied product) under the conditions of specific influences on the product. In the process of measurement, the product is subjected to the effects of vibration on the vibration test bench, and the implementation of this measurement method allows for solutions to a number of design problems, such as ensuring the required rigidity of structural elements under certain external influences. The required minimum frequency of measuring an information update is about 10 kHz and the measured object, in this case, makes linear-angular movements in all directions with the approximate ranges of its linear fluctuations within 3 mm and angular deviations within 2°. The specified limitations are determined by the requirements for the test conditions of the products. It is necessary to form a sequence of values for the angular deviations of the plane at each moment of measurement (not less than 10 thousand samples per second), with the minimum possible error of measurement as the result of the measurements.

2. Materials and Methods

2.1. Measuring Method

Based on the existing technical requirements of the measurement process, it is impossible to use contact methods of measurement due to the inability to standardize the measuring force under vibration conditions. The use of measuring systems based on CCD matrices (photo and video cameras) is not possible due to the high requirements for the frequency of measuring data updates (not less than 10 kHz) and, in the case of using high-speed cameras, the resolution of these cameras decreases significantly and the cost of the system increases extremely.

It is useful to convert the measurement information into the angular position of the laser beam directed outward from the target item by placing a reflector or light source on the monitored surface. The laser beam is distributed as a conditionally flat wave with an extremely small divergence angle of its light beam, which makes it possible to examine the laser beam projections at different distances. Interferometer-based systems (e.g., Michelson scheme) or high-speed photodetectors [6,7] for determining the spatial distribution of light on a diode surface (quadrant split photodiodes—QPD) can be used as alternative variants of sensing elements to determine the linear-angle position of the beam in space.

The interferometer allows for a registration of the change in the geometric path of the laser beam with a high speed and accuracy, but not the angular deviation of the beam. In order to perform the set task using the interferometer, three beams would be required to form three reference points on the plane under investigation. This makes both the design of the measurement system and the algorithm for processing the measurement information very difficult, which would also lead to high system implementation costs, since three interferometers (one for each of the beams) with sophisticated high-precision optics are required.

The use of QPD to solve the problems of measuring the angular deviation of a laser beam has been widely described in the literature [8–10], but there is one limitation that authors have not described. For example, in the implementation of the atomic force microscope circuit (Figure 1), the nano-movements of the cantilever Δx are converted into the angular deviation of the laser beam α by projecting the beam onto the back mirror surface of the cantilever. The reflected beam falls on the QPD, which registers the power of the light flux coming to each of the four photosensitive segments and, using a calculation of the pair differences of the readings, information is received about the displacement of the spot center of the laser beam projection, relative to the center of the QPD in the photodiode′s coordinate system. In this case, it is essential that the mirrored back surface of the cantilever is a console, one end of which is rigidly fixed in the device body, making linear movements of the mirrored surface essentially impossible. In the measurement problem described in the present article, linear movements of the surface under study are possible along all the axes, in connection with which, the use of the widespread measurement scheme with one QPD is not possible, because a linear displacement of the laser beam without changing its angular position will lead to a shift in the projection spot on the QPD surface, which will be falsely interpreted as an angular deviation.

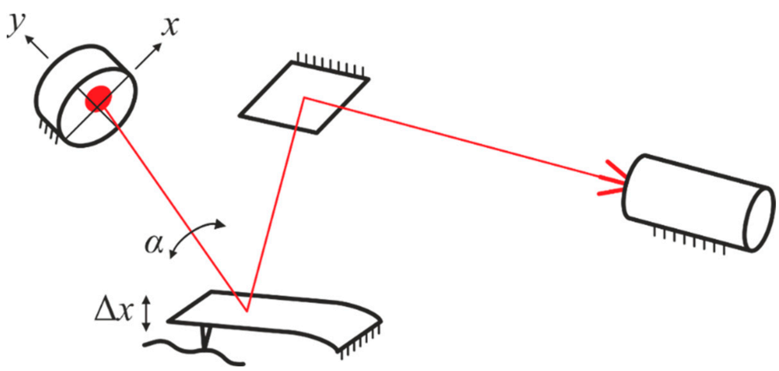

Figure 1. Scheme for measuring the angular deviation of a laser beam in an atomic force microscope.

To solve this problem, the authors propose the use of approaches close to photogrammetry [11,12]: using two beam projections (Figure 2) to determine the spatial location of the light source, including linear (x, y, z) and angular deviations (α_x, α_y, α_z) in the global coordinate system (X, Y, Z), using the coordinates of two projections (x′, y′ and x″, y″) in the QPDs coordinate systems, (X′, Y′) and (X″, Y″), respectively.

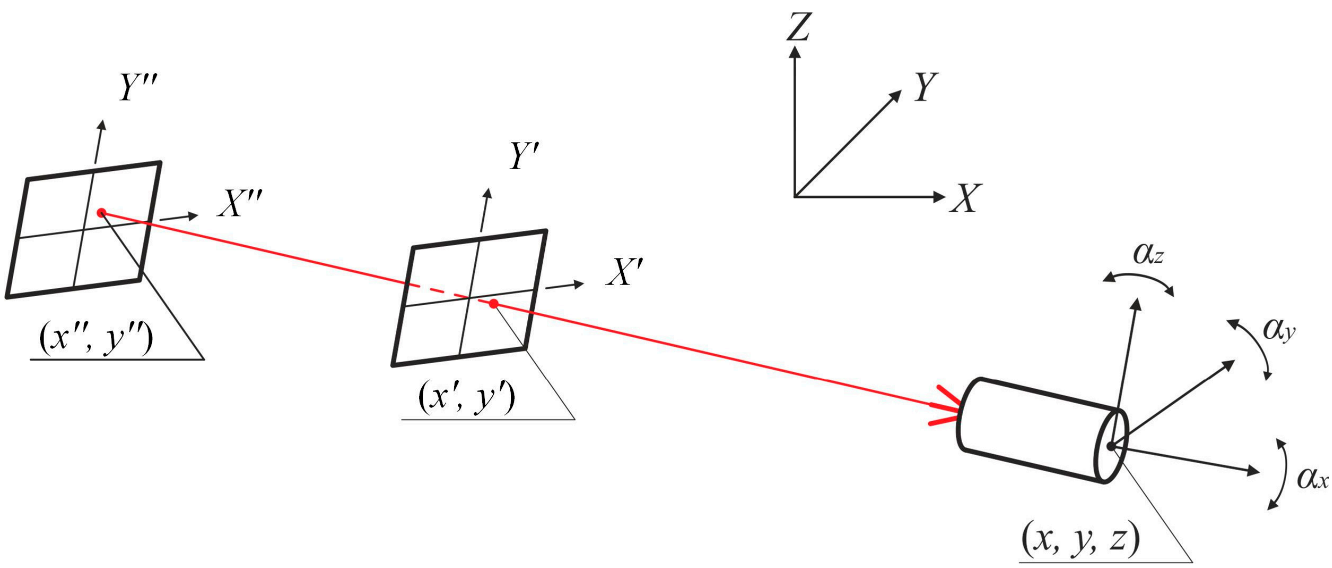

Figure 2. Laser beam trace in two projection planes.

2.2. Measurement Circuit Diagram

In the measurement scheme proposed by the authors (Figure 3), a laser diode, using a fixture, is attached to the studied plane of the part and the laser beam is oriented along the normal to the surface, which falls onto the beam-splitter cube, where it splits into two parts [13], each of which hits the QPD [14], located at a different distances from the beam-splitter cube.

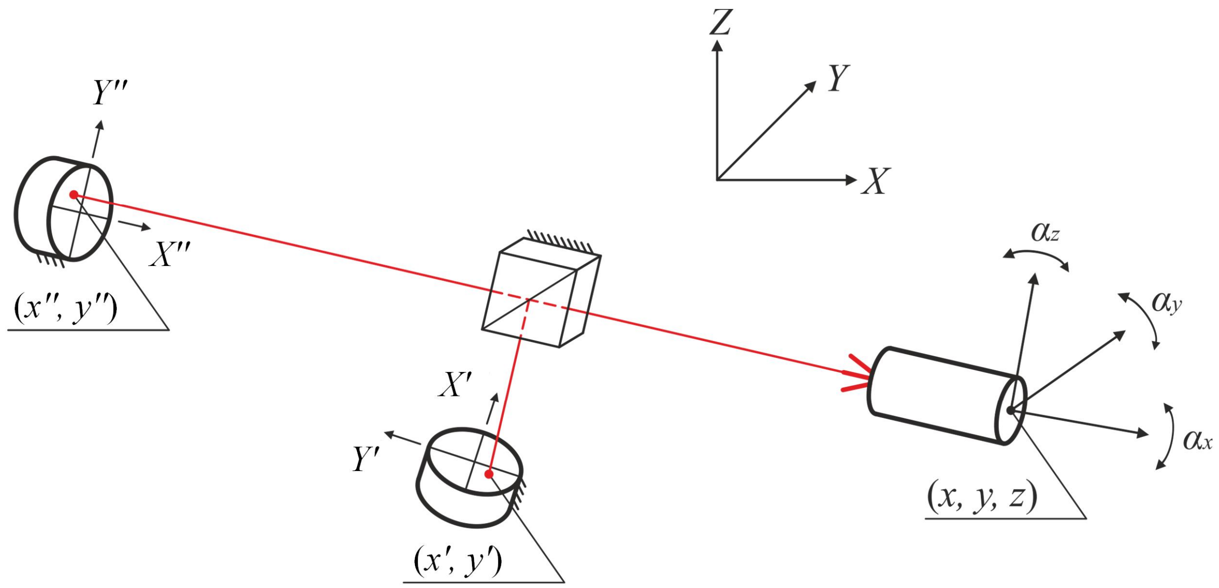

Figure 3. Schematic diagram of the proposed measuring system.

Thus, each of the photodiodes implements the projection plane of the laser beam, and the difference in the distances from each of the QPDs to the light-splitting cube is the distance between the projection planes.

The presented approach is sensitive to both linear and angular displacements of the laser source in all directions. To determine the deviation value, it is necessary to measure the deviation of the laser spot projections on the plane of each of the QPDs [15,16] in the QPD coordinate systems (X′, Y′ and X″, Y″), and then recalculate them into the angular deviation value, relative to some position taken as the initial one, in accordance with the mathematical model of the system [17].

2.3. Mathematical Model

To determine the effective distance from the measurement object to the sensitive elements (QPD), it is necessary to determine the zone of the QPD's sensitivity and the value of possible angular deviations, as dictated by the set task. As a base model, it is reasonable to proceed from the characteristics of the QPD (in the model chosen by the authors, the diameter of the sensitive zone of the photodiode is 9 mm), and also from the approximate distance from the farthest photodiode to the object of measurement (about 150–200 mm). Based on the geometry [18,19] of the measurement scheme with zero initial deviation in the laser beam center projection, the following dependence between the deviation in the laser beam projection center from the center of the QPD δ, the distance from the QPD to the measurement object L, and the angle of deviation in the laser beam from the initial (zero) position α can be used:

$$\alpha(\delta, L) = \frac{180}{\pi} \cdot atan\left(\frac{\delta}{L}\right); \tag{1}$$

Taking into view the given relations, when using the laser beam with a beam diameter of 4 mm (at values smaller than half of the QPD diameter, the range of limiting deviations will be limited by the diameter of the laser beam), the maximum deviation in the laser beam projection center from the photodiode center δ from relation (1), provided that the laser beam is completely placed in the sensitive area of the QPD and the projection is present in each of the four quadrants of photodiode, will be −2 mm. Thus, given the value of the maximum linear deviation in the laser beam projection center from the center of the QPD, the dependence of the angular deviation in the beam on the distance between the farthest QPD and the object of measurement is given (Figure 4).

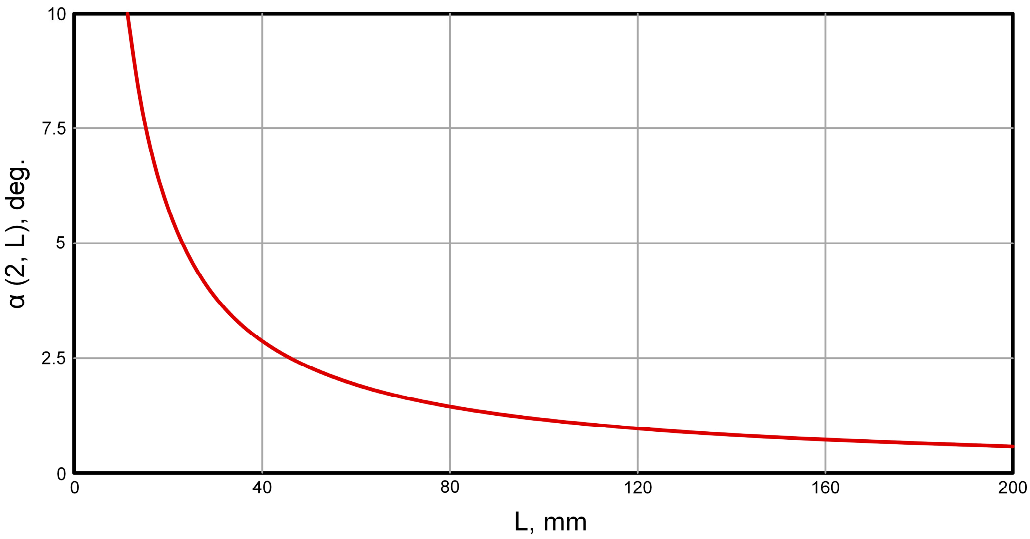

Figure 4. Angle of deviation α of the laser beam from the initial position depending on the distance between the QPD and the object of measurement.

The above calculations and dependencies are intended to illustrate the orders of values and dependencies between them.

Taking into account the physical principles of silicon photodiodes, it should be kept in mind that the output voltage of the photodiode segment is proportional to the surface area of the QPD segment illuminated by the light beam. Thus, the characteristics of the output voltage of the photodiode segments depend on the laser beam shape.

Taking into account the circular shape of the laser beam cross-section, it is possible to determine the expressions for the regions covered by the laser beam for each part of the QPD segments (Figure 5). For this purpose, it is first necessary to determine the equations for the upper and lower half-circle of the laser spot:

$$\begin{aligned} y_{Ru}(x, xc, yc, d) &= yc + \sqrt{\left(\tfrac{d}{2}\right)^2 - (x - xc)^2}; \\ y_{Rd}(x, xc, yc, d) &= yc - \sqrt{\left(\tfrac{d}{2}\right)^2 - (x - xc)^2} \end{aligned} \tag{2}$$

where $y_{Ru}(x,\ xc,\ yc,\ d)$ is the contour function of the upper half-circle of the laser beam projection spot, $y_{Rd}(x,\ xc,\ yc,\ d)$ is the contour function of the lower half-circle of the laser beam projection spot, xc and yc are coordinates of the center of the laser beam projection spot in the X', Y' coordinate system (Figure 5), and d is the diameter of the laser beam projection spot.

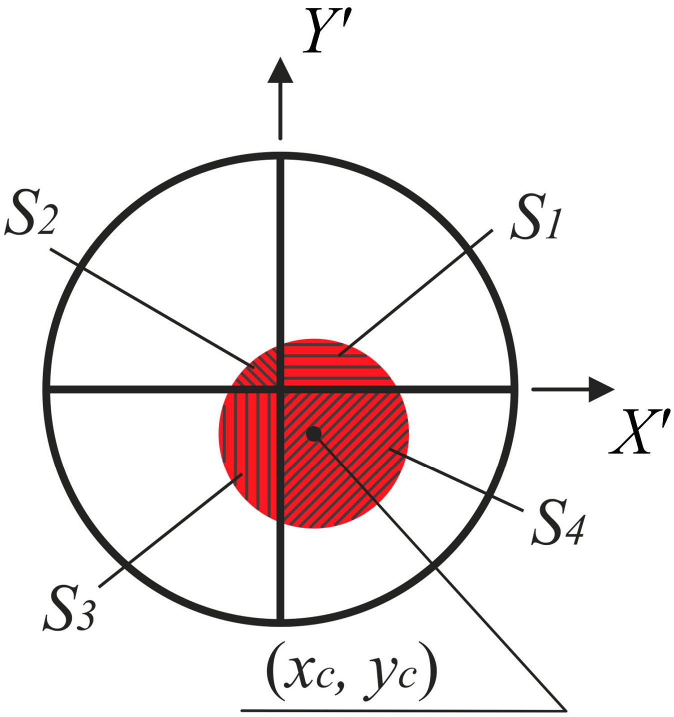

Figure 5. Projection of a circular laser beam onto photodiode segments.

Then, the surface areas of the QPD segments illuminated by the laser beam, depending on the coordinates of the spot center of the laser beam projection and spot diameter, take the look:

$$\begin{aligned} S_1(xc,yc,d) &= \int_0^{xc+\frac{d}{2}} y_{Ru}(x,xc,yc,d)dx - \int_0^{xc+\frac{d}{2}} y_{Rd}(x,xc,yc,d)dx,\ when\ y_{Ru} \geq 0\ and\ y_{Rd} \geq 0; \\ S_2(xc,yc,d) &= \int_{xc-\frac{d}{2}}^{0} y_{Ru}(x,xc,yc,d)dx - \int_{xc-\frac{d}{2}}^{0} y_{Rd}(x,xc,yc,d)dx,\ when\ y_{Ru} \geq 0\ and\ y_{Rd} \geq 0; \\ S_3(xc,yc,d) &= \int_{xc-\frac{d}{2}}^{0} y_{Ru}(x,xc,yc,d)dx - \int_{xc-\frac{d}{2}}^{0} y_{Rd}(x,xc,yc,d)dx,\ when\ y_{Ru} \leq 0\ and\ y_{Rd} \leq 0; \\ S_4(xc,yc,d) &= \int_0^{xc+\frac{d}{2}} y_{Ru}(x,xc,yc,d)dx - \int_0^{xc+\frac{d}{2}} y_{Rd}(x,xc,yc,d)dx,\ when\ y_{Ru} \leq 0\ and\ y_{Rd} \leq 0; \end{aligned} \tag{3}$$

Figure 6 shows three-dimensional value graphs of the photodiode segments' surface areas, covered by a spot of laser beam projection, depending on the coordinates of the spot center xc, yc at d = 4 mm. The signals at the output of the QPD segments will be proportional to the values of the areas covered by the spot of the laser beam projection and, as follows from relations (2) and (3), will have a non-linear character of change.

With voltage signals at the photodiodes output, which are proportional to the areas of the QPD segments covered by the spot of the laser beam projection, it is possible to determine the estimated coordinates of the center of the laser beam projection on the QPD plane, using the well known relations:

$$\begin{aligned} xc' &= U_1 + U_4 - U_2 - U_3; \\ yc' &= U_1 + U_2 - U_4 - U_3; \end{aligned} \tag{4}$$

where xc' and yc' are the estimated coordinates of the center of the laser beam projection on the photodiode plane, and U_1, U_2, U_3, and U_4 are the measurement signals (digitized values of the voltages of the corresponding QPD segments, numbering according to Figure 5).

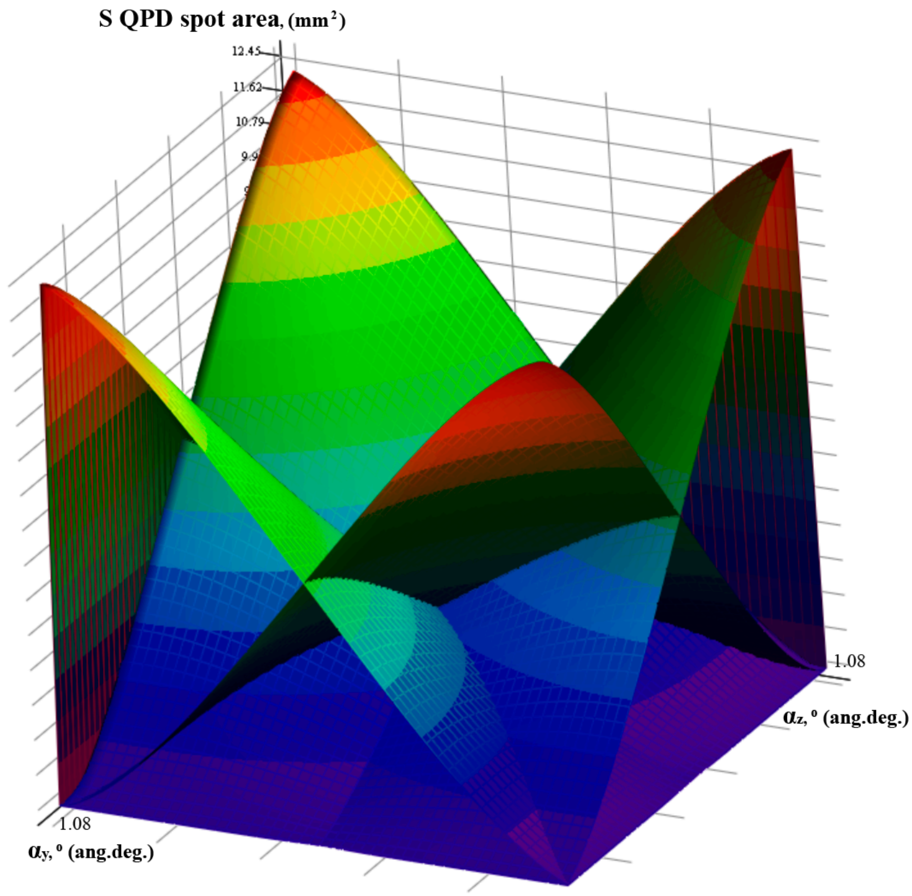

Figure 6. Diagrams of changes in the areas of the QPD segments covered by the laser beam projection spot depending on the coordinates of the center of the laser beam projection spot *xc*, *yc*.

In this case, xc and yc will differ from xc' and yc' due to the nonlinearity of Expressions (2) and (3), which can be further corrected using the total conversion function [20]. Given that, according to the measurement scheme (Figure 3), a pair of photodiodes located at different distances from the light source along the laser beam path is used to determine the total angular deviation α of the laser beam from its initial position, there are, in fact, two pairs of measuring signals (one each from QPD 1 and QPD 2), which can be recalculated according to Expression (4) into two pairs of estimated coordinates for the projection centers (xc', yc', xc'', yc'') of the laser beam on the planes of photodiode 1 and photodiode 2.

Thus, it is necessary to establish the relation between the estimated coordinates of the laser beam projection centers (xc', yc', xc'', yc'') and the total angle of deviation α of the laser beam from some initial (zero) position, nominally orthogonal to the planes of both QPDs, at which, the beam passes through the centers of both QPDs. Based on the results of empirical studies, the authors propose the following function for the total angle depending on the values of the two pairs of the projection centers' estimated coordinates:

$$\alpha\left(xc', yc', xc'', yc''\right) = k_0 \cdot \sqrt{\left(k_{11} \cdot xc'' - k_{12} \cdot xc' + b_1\right)^2 + \left(k_{21} \cdot yc'' - k_{22} \cdot yc' + b_2\right)^2}; \quad (5)$$

where α is the total angle of deviation in the laser beam initial position, xc', yc', xc'', and yc'' are coordinates of the laser beam projection centers in the projection planes of two slit photodiodes, k_0 is the scale factor conditioned by the laser beam diameter, k_{11}, k_{12}, k_{21}, and k_{22} are scale factors, which are responsible for the linear distortions at the registration of the coordinates of the laser beam projections, such as a deviation in the photodiodes normals from the nominal mutually orthogonal location, and b_1 and b_2 are linear displacement coefficients along the QPD axes, which are responsible for the deviation in the photodiodes' coordinate centers from the nominal location in the normal plane. The coefficients k_0, k_{11}, k_{12}, k_{21}, k_{22}, b_1, and b_2 are determined via a calibration of the measuring system.

3. Results and Discussion

3.1. Experimental Stand

In order to verify the theoretical statements outlined in the second section of this paper, the authors developed an experimental stand consisting of two quadrant segmented photodiodes (vendor OSI model SPOT-9DMI) and a light-splitting cube (model GCC-401112). A laser diode was used as a source of laser emission with a wavelength of 635 nm, a transmitter power of 5 mW, and a spot diameter at a distance of 100–200 mm in the range of 3.5–4 mm. The scheme included a current-limiting resistor of 88 ohms to reduce the intensity of the light radiation in connection with the limitations imposed by the manufacturer of the QPD.

Quadrant segmented photodiodes with a sensing zone diameter of 9 mm and a response time of less than 10 ns were use and the QPDs were included in a photovoltaic circuit. To digitize the signals [21] of the photodiodes, an internal 12-bit ADC of an 8-bit microcontroller [22], with an internal eight-channel multiplexer [23] and the strapping of the signal lines with capacitors with a 0.1 μF rating, was used. An external high-speed Flash memory circuit with a nominal volume of 64 Mbit was used to realize high-speed sensor polling with a rate above 10,000 samples per second.

The experimental stand is shown in Figure 7; the body of the experimental bench was created using the SLS-printing method from polyamide. The simulator was connected to a personal computer using the USB 2.0 or a higher interface with a hardware USB-UART bridge.

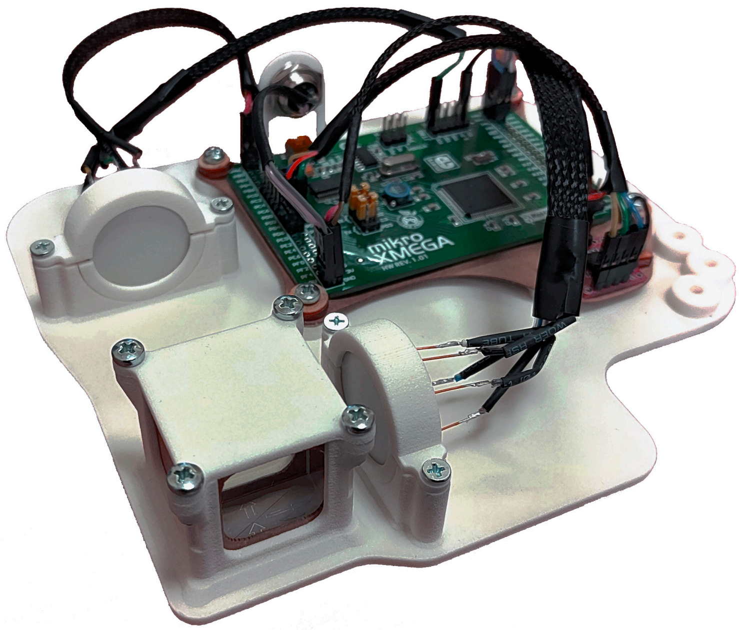

Figure 7. Photo of the measuring system stand.

3.2. Software and Calibration

To collect and evaluate the measurement information [24], special software was developed in C++ language and the software component of the system contained two parts:

- The microprogram of the microcontroller [25];

- Software for the personal computer;

The algorithm of the microcontroller′s work was built using the logic of the finite automata theory and the control was created by sending control commands from the computer; thus, the system had several working modes:

- High-speed data acquisition (cyclic digitalization of sensor output signals from eight channels, which were recorded into external memory until it was full);

- Data transfer to computer via USB interface (complete transfer of all the recorded data from the external memory—more than 700 thousand records);

- System calibration (transfer of current sensor readings directly to the computer at a low speed for the calibration and calculation of the Equation (5) coefficients);

- Idle mode;

The interface of the computer program was realized in the format of a single-window application, implementing graphic images of the QPD′s center crosses by drawing in them the laser beam projections and calculations of the coordinates of the laser beam projection centers. The mode of the data collection from the external memory of the stand, which was recorded in a text file for the subsequent analysis, was realized as an independent thread.

The main target of the calibration process was determining the internal parameters of the system, k_0, k_{11}, k_{12}, k_{21}, k_{22}, b_1, and b_2, from Expression (5). To calibrate the system, it was necessary to provide a laser beam falling with a number of known angles α and to fix the values of xc', yc', xc'', and yc'' for each α angle. With at least seven described data sets, it was possible to solve the obtained system of equations relative to the required coefficients k_0, k_{11}, k_{12}, k_{21}, k_{22}, b_1, and b_2, and increasing the number of data sets made possible to solve the system with control, reducing the calibration error via an application of LSM or other solution search methods.

An important characteristic of the calibration process was the necessity of maintaining a certain location of the laser beam projection centers in the QPDs' planes; the best solution was a uniform distribution over the entire surface or a distribution with increasing density as one approached the QPD centers. To set exemplary influences (known values of angular deviation α), the authors developed a device to place the light source on the working surface of the coordinate-measuring machine. After committing the micro-movements of the beam [26], the angle was determined by the coordinate-measuring machine as a position of the precise cylinder based in a device rigidly connected to the laser transmitter.

3.3. Experimental Results

Based on the results of the simulation, the authors determined the optimal number of data sets for the calibration to be equal to nine. Their arrangement, with the total distribution of the theoretical measurement error within $\pm 1''$ (one angular second) and the reference angles of the beam direction deviation relative to the initial position (orthogonal to the photodiode planes), was $0°$; $\pm 0.345°$; and $\pm 0.53°$ when the laser beam rotated alternately in two mutually orthogonal directions (α_y pitch and α_z yaw).

The error map is shown in Figure 8, with the laser beam angular deviation limits being in each of the two mutually orthogonal directions (α_y pitch and α_z yaw) of $\pm 0.764°$ and about 75% of the error map falling within $\pm 1''$. The remaining 25% of the measurement range could also be used, but with a correction for a larger measurement error value. It is necessary to notice that the resulting values of the limits of the measurements of the angular deviations did not include all the possibilities of the obtained measuring system, so if the distance from a far-end QPD to the investigated object was reduced from the nominal value of 150 mm used by authors, it was possible to receive measuring ranges of angular deviations up to $10°$. It was also possible to increase the measuring range of the instrument using special wide-angle lenses that allowed for an increase in the range of the deviations in the input beams, but the measurement error would be increased and would most likely change the character of the distribution, which would require additional recalculations. In addition to using special optical lenses, it was possible to increase the sensitivity range of the sensors (QPD) by using scattering matte glasses, which made the intensity distribution of the laser beam incident be on the sensor smoother. These variants in the modifications of the measuring system are a subject of interest and will undoubtedly be carried out in the future.

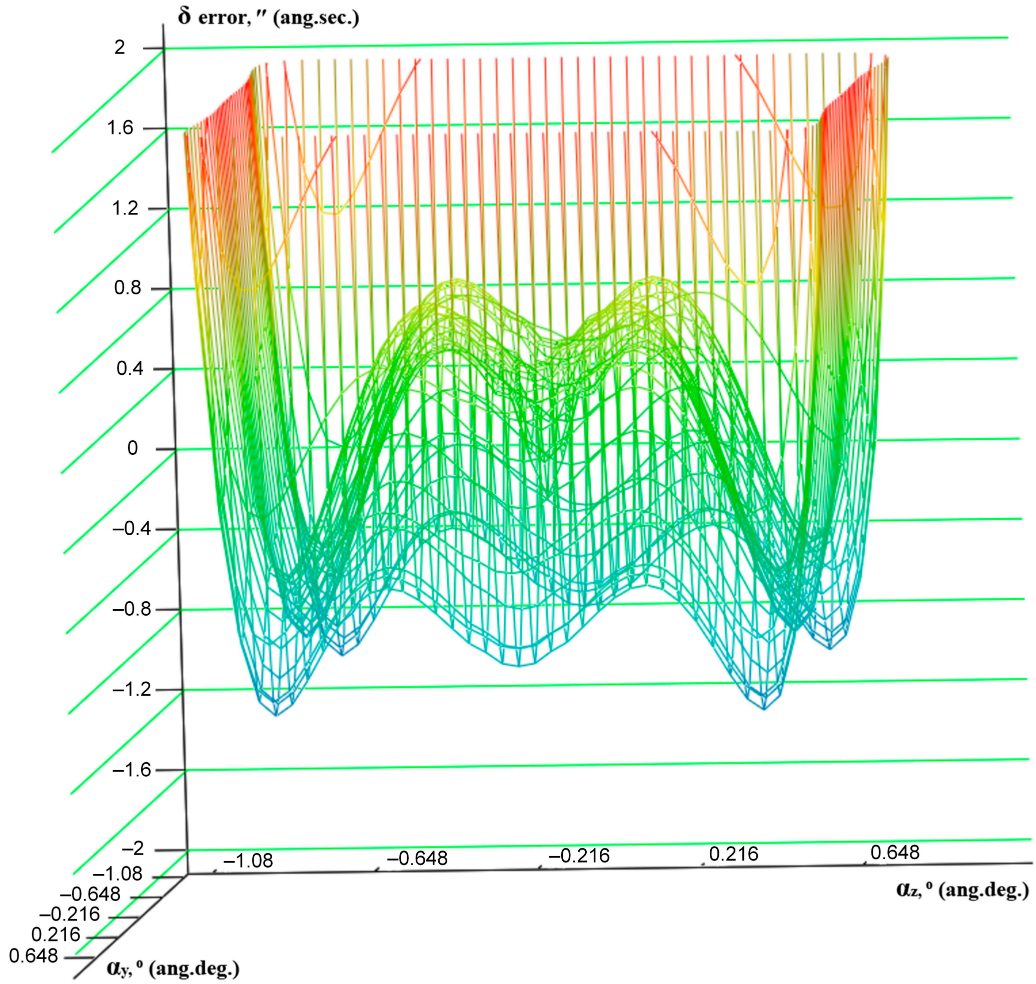

Figure 8. Measuring system error map.

According to the results of the experiments implemented by authors, on the created and calibrated stand, it was possible to achieve a relative error of measurement over the entire measurement range (which was around ±5° on an experimental stand made by authors) within 2%, and in the central part, up to 0.5%.

4. Conclusions

The authors proposed a scheme for measuring the angular deviation in critical machinery product surfaces in dynamic mode (including measurements performed during tests under conditions close to operating conditions). The described solution, in contrast to similar and widely known methods, was not sensitive to linear displacements of the light source along all the axes and allowed for controlling the rotation of the examined surface in all directions. Depending on the task, the measurement ranges could vary [27] from fractions of a degree to tens of degrees, and the error of measurement [28] from the units of the angular seconds to fractions of a degree. The most important advantage of the proposed system was the use of a laser beam as a carrier of measuring information and a pair of QPDs as a receiver, which made it possible to achieve a high frequency of interrogation in the measuring system (tens of thousands samples per second). One of the important applications of the obtained results is the use of real-time measurement results as feedback for CNC systems [29,30]. The authors have outlined further directions for the development of the research; they plan to develop new modifications for the measuring system, allowing for the achievement of a larger measurement range and less sensitivity to external measurement conditions, with a preservation of the orders of the measurement error range.

Author Contributions: Conceptualization, S.K.; methodology, S.G.; software, S.K.; validation, S.G.; formal analysis, P.S.; investigation, A.F.; resources, P.P.; data curation, A.F.; writing—original draft preparation, S.K.; writing—review and editing, P.P.; visualization, S.K.; supervision, S.K.; project administration, S.G.; funding acquisition, P.S. All authors have read and agreed to the published version of the manuscript.

Funding: This research was funded by Ministry of Science and Higher Education of the Russian Federation, project number FSFS-2021-0003.

Institutional Review Board Statement: Not applicable.

Informed Consent Statement: Not applicable.

Data Availability Statement: Data underlying the results presented in this paper are not publicly available at this time but may be obtained from the authors upon reasonable request.

Acknowledgments: The work was carried out on the equipment of the Collective Use Center of MSTU "STANKIN" (project No. 075-15-2021-695).

Conflicts of Interest: The authors declare no conflict of interest.

Nomenclature

Abbreviation	Description
CCD	Charge-coupled device
QPD	Quadrant segmented photodiode
ADC	Analog to digital converter
LSM	Least square method
CNC	Computer numeric control

References

1. Gao, W.; Kim, S.W.; Bosse, H.; Haitjema, H.; Chen, Y.L.; Lu, X.D.; Knapp, W.; Weckenmann, A.; Estler, W.T.; Kunzmann, H. Measurement technologies for precision positioning. *CIRP Ann.* **2015**, *64*, 773–796. [CrossRef]
2. Su, X.; Zhang, Q. Dynamic 3-D shape measurement method: A review. *Opt. Lasers Eng.* **2010**, *48*, 191–204. [CrossRef]
3. Konov, S.G. Mobile contact-type coordinate-measurement system based on a photogrammetric system. *Meas. Tech.* **2010**, *53*, 149–152. [CrossRef]
4. Khuc, T.; Catbas, F.N. Computer vision-based displacement and vibration monitoring without using physical target on structures. *Struct. Infrastruct. Eng.* **2017**, *13*, 505–516. [CrossRef]
5. Fan, W.; Qiao, P. Vibration-based Damage Identification Methods: A Review and Comparative Study. *Struct. Health Monit.* **2011**, *10*, 83–111. [CrossRef]
6. Cincotta, S.; Neild, A.; He, C.; Armstrong, J. Visible Light Positioning Using an Aperture and a Quadrant Photodiode. In Proceedings of the IEEE Globecom Workshops (GC Wkshps), Singapore, 4–8 December 2017; pp. 1–6.
7. Chong, K.K.; Yew, T.K. Novel Optical Scanner Using Photodiodes Array for Two-Dimensional Measurement of Light Flux Distribution. *IEEE Trans. Instrum. Meas.* **2011**, *60*, 2918–2925. [CrossRef]
8. Song, Y.; Bhushan, B. Atomic-scale topographic and friction force imaging and cantilever dynamics in friction force microscopy. *Phys. Rev. B* **2006**, *74*, 165401. [CrossRef]
9. Klochkova, V.; Sheldakova, J.; Galaktionov, I.; Nikitin, A.; Kudryashov, A.; Belousov, V.; Rukosuev, A. Local Correction of the Light Position Implemented on an FPGA Platform for a 6 Meter Telescope. *Photonics* **2022**, *9*, 322. [CrossRef]
10. Kudryashov, A.; Alexandrov, A.; Rukosuev, A.; Samarkin, V.; Galarneau, P.; Turbide, S.; Châteauneuf, F. Extremely high-power CO2 laser beam correction. *Appl. Opt.* **2015**, *54*, 4352–4358. [CrossRef]
11. Konov, S.G.; Krutov, A.V. Development of a system for tracking the spatial movements of objects based on the technology of photogrammetry. *Meas. Tech.* **2014**, *56*, 1386–1389. [CrossRef]
12. Riveiro, B.; González-Jorge, H.; Varela, M.; Jauregui, D.V. Validation of terrestrial laser scanning and photogrammetry techniques for the measurement of vertical underclearance and beam geometry in structural inspection of bridges. *Measurement* **2013**, *46*, 784–794. [CrossRef]
13. Rayas, J.A.; León-Rodríguez, M.; Martínez-García, A.; Genovese, K.; Medina, O.M.; Cordero, R.R. Using a single-cube beam-splitter as a fringe pattern generator within a structured-light projection system for surface metrology. *Opt. Eng.* **2017**, *56*, 044103. [CrossRef]
14. Roa, J.; Oncins, G.; Diaz, J.; Sanz, F.; Segarra, M. Calculation of Young's Modulus Value by Means of AFM. *Recent Pat. Nanotechnol.* **2011**, *5*, 27–36. [CrossRef] [PubMed]
15. Ishola, F.; Cho, M. Experimental Study on Photodiode Array Sensor Aided MEMS Fine Steering Mirror Control for Laser Communication Platforms. *IEEE Access* **2021**, *9*, 100197–100207. [CrossRef]

16. Zečević, N.; Hofbauer, M.; Goll, B.; Zimmermann, H.; Tondini, S.; Chalyan, A.; Fontana, G.; Pavesi, L.; Testa, F.; Stracca, S.; et al. A 3D Photonic-Electronic Integrated Transponder Aggregator with 48 × 16 Heater Control Cells. *IEEE Photonics Technol. Lett.* **2018**, *30*, 681–684. [CrossRef]
17. Iosifidis, D.; Koivisto, T. Scale Transformations in Metric-Affine Geometry. *Universe* **2019**, *5*, 82. [CrossRef]
18. Du, Z.-G.; Pan, J.-S.; Chu, S.-C.; Luo, H.-J.; Hu, P. Quasi-Affine Transformation Evolutionary Algorithm with Communication Schemes for Application of RSSI in Wireless Sensor Networks. *IEEE Access* **2020**, *8*, 8583–8594. [CrossRef]
19. Meng, Z.; Pan, J.-S.; Xu, H. QUasi-affine transformation evolutionary (QUATRE) algorithm: A cooperative swarm based algorithm for global optimization. *Knowl-Based Syst.* **2016**, *109*, 104–121. [CrossRef]
20. Dong, H.-W.; Su, X.-X.; Wang, Y.-S.; Zhang, C. Topological optimization of two-dimensional phononic crystals based on the finite element method and genetic algorithm. *Struct. Multidiscip. Optim.* **2014**, *50*, 593–604. [CrossRef]
21. Jaanus, M.; Udal, A.; Kukk, V.; Umbleja, K. Using Microcontrollers for High Accuracy Analogue Measurements. *Elektron. Ir Elektrotech.* **2013**, *19*, 51–54. [CrossRef]
22. Grigoriev, S.N.; Martinov, G.M. An ARM-based Multi-channel CNC Solution for Multi-tasking Turning and Milling Machines. *Procedia CIRP* **2016**, *46*, 525–528. [CrossRef]
23. Sharma, M.; Agarwal, N.; Reddy, S.R.N. Design and development of daughter board for USB-UART communication between Raspberry Pi and PC. In Proceedings of the International Conference on Computing, Communication & Automation, Greater Noida, India, 15–16 May 2015; pp. 944–948.
24. Grigoriev, S.N.; Emelianov, P.N.; Masterenko, D.A.; Ped', S.E. Sampling by Variables for Rayleigh Distributed Lots. *Meas. Tech.* **2022**, *65*, 417–425. [CrossRef]
25. Barrett, S.F.; Pack, D.J. Microchip AVR Operating Parameters and Interfacing. In *Microchip AVR Microcontroller Primer: Programming and Interfacing*; Synthesis Lectures on Digital Circuits & Systems; Springer: Berlin/Heidelberg, Germany, 2019.
26. Gao, W.; Shi, H.; Tang, Q. A Contactless Planar Inductive Sensor for Absolute Angular Displacement Measurement. *IEEE Access* **2021**, *9*, 160878–160886. [CrossRef]
27. Goyal, D.; Pabla, B.S. The Vibration Monitoring Methods and Signal Processing Techniques for Structural Health Monitoring: A Review. *Arch. Comput. Methods Eng.* **2016**, *23*, 585–594. [CrossRef]
28. Grigoriev, S.N.; Masterenko, D.A.; Teleshevskii, V.I.; Emelyanov, P.N. Contemporary state and outlook for development of metrological assurance in the machine-building industry. *Meas. Tech.* **2013**, *55*, 1311. [CrossRef]
29. Grigoriev, S.N.; Martinov, G.M. The Control Platform for Decomposition and Synthesis of Specialized CNC Systems. *Procedia CIRP* **2016**, *41*, 858–863. [CrossRef]
30. Grigoriev, S.N.; Martinov, G.M. Research and development of a cross-platform CNC kernel for multi-axis machine tool. *Procedia CIRP* **2014**, *14*, 517–522. [CrossRef]